Influence of Steel Manufacturing on J-A Model Parameters and Magnetic Properties

Babak Vaseghi, Shah Asifur Rahman, and Andrew M. Knight

Department of Electrical & Computer Engineering, University of Alberta, Edmonton, Alberta, Canada

The influence that manufacturing processes have on electrical steel properties is investigated. The investigation is carried out by considering changes in measured electromagnetic quantities and the changes to parameters of a physics-based hysteresis model. The parameters of an inverse Jiles–Atherton hysteresis model are identified using nonlinear least square method and compared with measured data from steel samples that have undergone different stages of manufacturing. The results of the study may be used as a first step to the inclusion of manufacturing effects in models of electromagnetic devices.

Index Terms—**Core loss, hysteresis, J-A model, magnetic properties, parameter identification, steel manufacturing.**

I. INTRODUCTION

NON-ORIENTED electrical steels are required for cheap, reliable and robust production of electrical machines. Progress to improve modeling of non-oriented electrical steels has involved fundamental aspects to obtain an accurate relationship between the field intensity and flux density that correctly accounts for hysteresis and eddy currents. Recently, there has been a growing interest in understanding the relationship between secondary manufacturing processes and magnetic properties, e.g. [1]–[5]. The performance and electromagnetic properties of non-oriented electrical steels are dependent on many different levels of structural detail, all related to their processing. Manufacturing processes such as casting, welding, cutting and annealing have all been shown to affect the performance of electrical steels. Knowledge of the effects of secondary manufacturing is one step towards being able to account for these effects during the design of electromagnetic devices. This paper continues the investigation of the relationship between secondary manufacturing and magnetic properties, while investigating the possibility of including those effects in a hysteresis model.

A number of hysteresis models are widely cited in the literature. For the work in this paper, considering the physical processes and the impact on electromagnetic quantities, a physics-based hysteresis model is desirable. The Jiles–Atherton (J-A) model [6] has physical significance and can be modified regarding to steel manufacture process and changes in the B-H curve. Furthermore, the J-A model is relatively simple to implement, with a known inverse model [7] and requires reasonable computational effort. Using a parameter identification algorithm with measured DC hysteresis curves, changes to the J-A model parameters are be tracked as a function of increased secondary manufacturing processing.

II. JILES–ATHERTON MODEL

The Jiles–Atherton model [6] describes a hysteretic magnetization curve in terms of the anhysteretic magnetization, irreversible magnetization and reversible magnetization. The governing equations of the J-A model are

$$\frac{dM}{dB} = \frac{(1-c)\frac{dM_{irr}}{dB_e} + \frac{c}{\mu_0}\frac{dM_{an}}{dH_e}}{1 + (1-\alpha)(1-c)\frac{dM_{irr}}{dB_e} + c(1-\alpha)\frac{dM_{an}}{dH_e}} \quad (1)$$

$$M_{an} = M_s\left[coth\frac{H_e}{a} - \frac{a}{H_e}\right] \quad (2)$$

$$\frac{dM_{an}}{dH_e} = \frac{M_s}{a}\left[1 - coth^2\frac{H_e}{a} + \left(\frac{a}{H_e}\right)^2\right] \quad (3)$$

$$M_{irr} = \frac{M - c.M_{an}}{1-c} \quad (4)$$

$$\frac{dM_{irr}}{dB_e} = \frac{(M_{an} - M_{irr})}{\mu_0 k\delta} \quad (5)$$

$$H_e = H + \alpha.M \quad (6)$$

In (1)–(6) M is magnetization, with M_{an} the anhysteretic magnetization, M_{irr} the irreversible magnetization and M_s the saturation magnetization; H denotes field intensity, with H_e the effective field intensity taking into account domain interactions; B is flux density with B_e the effective flux density. Including M_s the five parameters specific to the J-A model are the anhysteretic behaviour parameter $a(A/m)$, the main field parameter α; the domain flexing constant c and the pinning parameter $k(A/m)$. The remaining variables in (1)–(6) are the directional parameter δ, which is ± 1 for dH/dt $\gtrless$ 0, and μ_0, the permeability of free space.

The identification of the five J-A model parameters from experimental measurement is a key point in the J-A model [8], [9]. A number of papers have considered this subject, e.g. [9]–[18]. For the work in this paper, the authors have found that a combination of nonlinear least squares fitting together with a pattern search algorithm provides consistent results. [18].

III. STUDY OF SECONDARY MANUFACTURING INFLUENCE

Secondary manufacturing processes can be defined as those manufacturing processes that steel is subjected to after delivery to the electric machine manufacturer. i.e. those undergone during the making of equipment, rather than those that are undergone in the process of actually making the electrical steel. For the purposes of this work, the secondary manufacturing processes that are considered are annealing, welding and interlocking.

TABLE I
SAMPLE LABELING

Name	Description
S0	SRA, no secondary manufacturing
N0	Non-SRA, no secondary manufacturing
SI-2, SI-4, SI-6	SRA: 2, 4, or 6 Interlocks
NI-2, NI-4, NI-6	Non-SRA: 2, 4, or 6 Interlocks
SW1-2, SW1-4, SW1-6	SRA: 2, 4 or 6 welds at depth 1
NW1-2, NW1-4, NW1-6	Non-SRA: 2, 4, or 6 welds at depth 1
SW2-2, SW2-4, SW2-6	SRA: 2, 4 or 6 welds at depth 2
NW2-2, NW2-4, NW2-6	Non-SRA: 2, 4, or 6 welds at depth 2

TABLE II
NON-SRA, J-A MODEL PARAMETERS

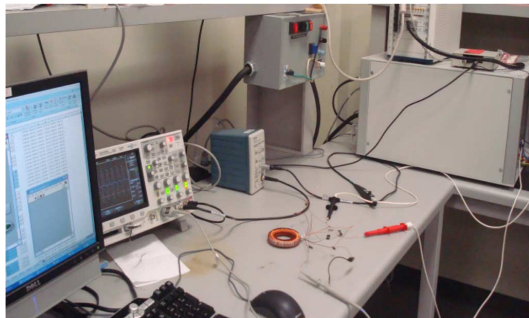| Sample	M_s(A/m)	a(A/m)	α	c	k(A/m)
N0	1.28E+06	351.9	7.73E-04	0.8438	330.0
NI-2	1.30E+06	448.9	9.47E-04	0.8043	262.0
NI-4	1.33E+06	577.7	0.0012	0.8599	404.6
NI-6	1.38E+06	760.9	0.0015	0.8788	474.7
NW1-2	1.28E+06	351.3	7.65E-04	0.7998	236.7
NW1-4	1.28E+06	349.2	7.51E-04	0.7441	177.8
NW1-6	1.28E+06	358.0	7.64E-04	0.5464	99.6
NW2-2	1.28E+06	331.1	7.15E-04	0.7546	184.2
NW2-4	1.29E+06	354.4	7.39E-04	0.688	151.1
NW2-6	1.29E+06	375.4	7.85E-04	0.7865	225.6

Fig. 1.　Experimental test workbench setup.

All the samples testing in this paper are nominally the same grade, 35X250, and are all from a single steel supplier. The samples under consideration are toroid samples, to enable the effects of welding to be investigated. The samples for testing are divided into two groups, those that are stress-relief annealed (SRA) and those that are not (non-SRA). The SRA process is carried out after the laminations have been punched but prior to welding or interlocking.

The toroid samples in the test have primary and secondary coils that are wound with a number of different taps, to enable measurements to be taken at a wide range of flux densities and frequencies. The samples are constructed with one of 0, 2, 4 or 6 interlocks or 0, 2, 4, or 6 welds, with 2 different weld depths considered. The interlocks are constructed such that each interlock has a length 1.8% of the mean flux path length and width equal to 35% of the flux path width. Weld depth 1 is 8.75% of the width of the flux path; weld depth 2 is 17.5% of the width of the flux path. The inside diameter of the toroid core is 0.85 of the outside diameter. For the purposes of identification in the following sections, the samples are labelled as defined in Table I.

Testing is carried out in accordance with standards ASTM A773-M and ASTM A927-M. The toroid test facility is shown in Fig. 1.

The test facility consists of a local computer with user interface; networked to a NI-PXI chassis running a LabView real-time system. The real-time system generates the excitation voltage waveforms, which are amplified using a linear amplifier with 100 V, 20 A peak output capability. Primary current and secondary voltage signals are recorded using an Agilent MSO 2004x oscilloscope. Tests on the toroid samples are conducted under quasi-static conditions (a 0.1 Hz triangular primary current waveform) to enable identification of the J-A waveform parameters and allow evaluation of the ability of the J-A model to accurately predict the waveform shape for

all samples. In addition tests are carried out at the following frequencies: 50 Hz, 60 Hz, 100 Hz, 200 Hz, 300 Hz, 400 Hz, 1 kHz, 2 kHz and 5 kHz. Coreloss data for a sample of these data points is presented

IV. J-A PARAMETER IDENTIFICATION AND DC RESULTS

The parameter identification method described in [21] is applied to the quasi-static magnetization curve measurements. Results in this section are grouped by whether or not the sample is annealed.

A. Non-SRA Samples

The variation of the J-A parameters for the non-SRA samples, as identified by the automated algorithm with nonlinear least squares and pattern search is presented in Table II. Considering the physical interpretation of the J-A model parameters, M_S, a and α control the shape of the anhysteretic magnetization curve; c is related to domain wall bulging and reversible magnetization, while k is related to irreversible magnetization due to domain wall movement past pinning sites. In [6] both c and k can be argued to be functions of pinning site density.

Considering first the interlocking process, additional punching is applied to the lamination to create the interlock. As a result additional residual stresses are to be expected in the region of the interlock, due to both the punching process and the assembly process. Observing the J-A parameters, one sees a progressive increase in the values of the parameters associated with the anhysteretic magnetization curve. This result is consistent with the demagnetizing effect of additional residual stresses in the sample. Considering the parameters that predict reversible and irreversible magnetization, the trend with increased secondary manufacturing is not consistent.

The measured BH loops for samples N0 and NI-6 are plotted in Fig. 2 together with those predicted by an inverse J-A model [7], [8]. In both the inverse model and the measurement, the initial magnetization and one full cycle at 1.5 T are presented. For case N0, the area enclosed by a full cycle of the prediction is 85% of the area enclosed by the measured loop. For case NI-6, the area enclosed by the prediction is 98% of the area enclosed by the measured loop. Considering the cases when welding is applied, the J-A parameters indicate that the anhysteretic curve is largely unchanged by the welding process. However, there are significant reductions in both k and c. These results imply that the welding process may impact pinning site density, possibly
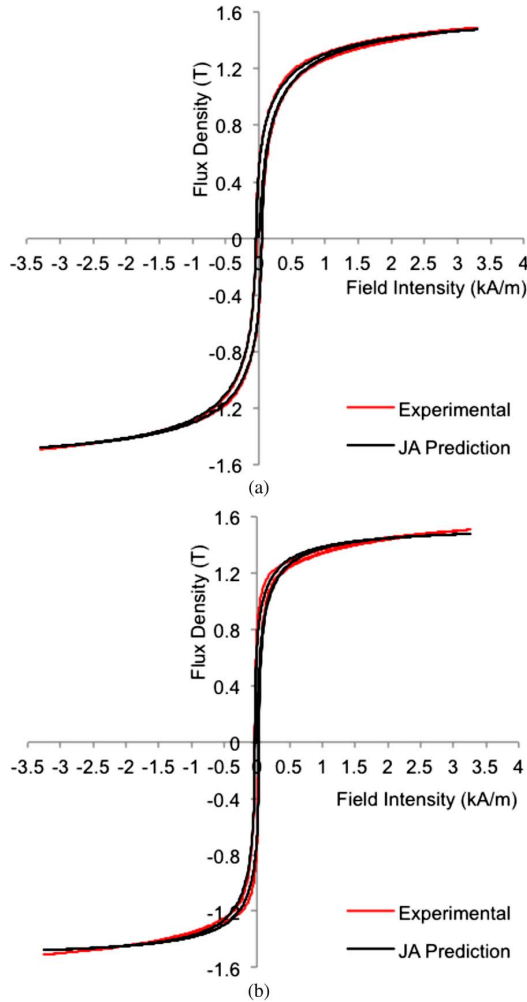
Fig. 2. Measured and predicted BH loops for example non-SRA samples. (a) Sample N0. (b) Sample NI-6.
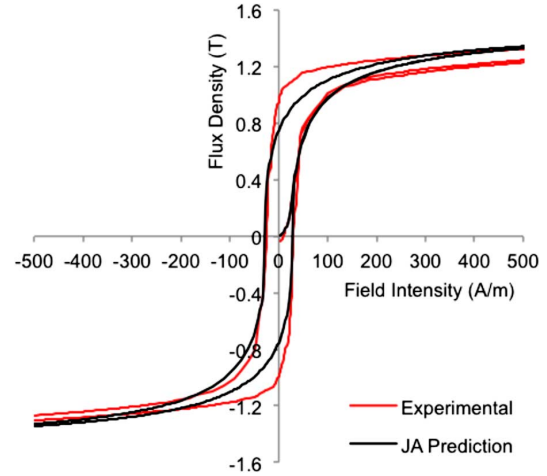

Fig. 3. Measured and predicted BH loops for SRA sample with no secondary manufacturing.

TABLE III
SRA, J-A MODEL PARAMETERS

	M_s(A/m)	a(A/m)	α	c	k(A/m)
S0	1.20E+6	81.2	1.99E-04	0.216	36.8
SI-2	1.20E+6	84.1	2.06E-04	0.8061	134.9
SI-4	1.22E+06	125.5	3.03E-04	0.6059	86.9
SI-6	1.22E+06	131.0	3.23E-04	0.7986	199.6
SW1-2	1.21E+06	107.1	2.64E-04	0.6535	99.3
SW1-4	1.23E+06	137.7	3.21E-04	0.3299	50.6
SW1-6	1.23E+06	156.3	3.63E-04	0.4201	55.1
SW2-2	1.23E+06	133.9	3.21E-04	0.7169	120.7
SW2-4	1.24E+06	184.3	4.22E-04	0.7336	130.6
SW2-6	1.29E+06	278.6	5.98E-04	0.7431	138.7

due to localized heating. However, the cause behind this observation is the subject of ongoing research.

1) SRA Samples: Automated identification of suitable J-A model parameters for the SRA samples is more difficult than for the non-SRA samples. Specifically, for sample S0, with SRA applied to a high-permeability low-loss steel, it is difficult to obtain J-A model parameters that are capable of accurately reflecting the sharp saturation knee observed in the measured data. Plots of the measured and best-fit inverse J-A model curves are shown in Fig. 3, with scale adjusted to show detail at low field intensity. It appears that the Langevin sigmoid function used to describe the anhysteretic magnetization is not capable of reproducing the rectangular hysteresis function with low coercive force that is observed in these measurements. The area enclosed by the best fit J-A curve is only 48% of the measured loop.

The quality of the J-A parameter fit to other SRA samples improves as the material is subject to secondary manufacturing and the hysteresis loop becomes less rectangular. Table III presents the J-A parameters identified for the SRA samples. In comparison with Table II, the J-A parameters a, α are smaller than the SRA samples, indicating that the anhysteretic curve has a sharper saturation knee. Unlike the non-SRA samples, the both the interlocked and welded samples show a progressive increase in a and α with increased secondary manufacturing.

V. IMPACT ON AC CORE LOSSES

As described earlier, the samples were tested to obtain values for AC core loss density. Data from these measurements is presented in Fig. 4, Fig. 5, and Fig. 6 for the interlocks, weld depth 1 and weld depth 2 respectively and frequencies from 60 Hz to 400 Hz. To enable side-side comparison across the frequency range, losses are presented in terms of % change relative to sample N0 at each frequency. In almost all cases, as one would expect, the SRA samples have lower measured loss than the corresponding non-SRA samples. However, the variation in losses due to secondary manufacturing is lower for the non-SRA samples. Considering the losses for the interlock samples in Fig. 4, the non-SRA samples show increasing loss with the number of interlocks. For SRA samples this trend is less clear; the 6-interlock sample exhibits lower loss than the 4-interlock sample. Considering Fig. 5 and Fig. 6, the results indicate that welding does not significantly impact the non-SRA losses, but does does significantly impact the losses in the SRA samples. Comparing the variations in losses with the J-A parameters in Table II and Table III, the trend of variations in losses with secondary manufacturing is most closely matched by variations in a and α. Specifically: 1) the non-SRA samples show little variation in these parameters with welding, and there is little observed variation in losses; 2) the SRA samples show an increase in these parameters with welding and there is an observed increase in losses; 3) both SRA and non-SRA show increases to a and
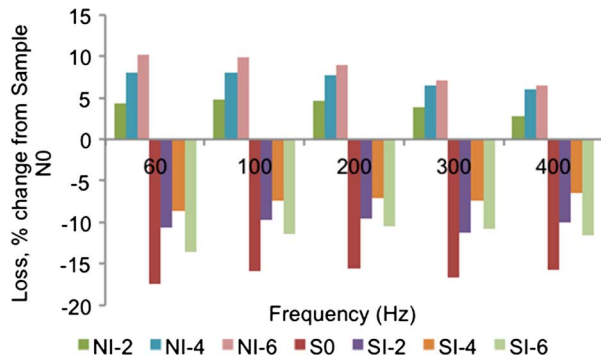
Fig. 4. Influence of interlocks on core loss at 1.5 T: % change in iron loss relative to the sample that has not been annealed and has no welds or interlocks.
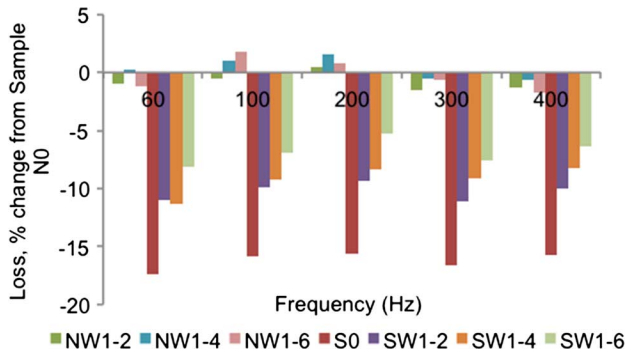

Fig. 5. Influence of welds at depth 1 on core loss at 1.5 T: % change in iron loss relative to the sample that has not been annealed and has no welds or interlocks.
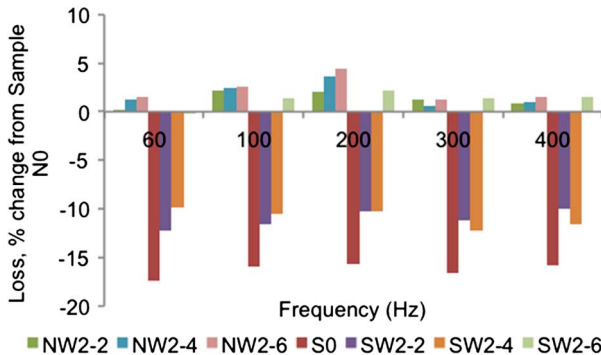

Fig. 6. Influence of welds at depth 2 on core loss at 1.5 T: % change in iron loss relative to the sample that has not been annealed and has no welds or interlocks.

α with interlocking, and there is an observed increase in loss. There does not appear to be a similar trend with c or k.

VI. CONCLUSION

The influence that secondary manufacturing processes have on measured DC hysteresis magnetization loops and AC core losses are presented. The measured hysteresis loops are used with a parameter identification algorithm to investigate the ability of an inverse J-A model to reflect the influence of manufacturing. Automated identification of parameters results in a high quality fit between measured and predicted curves for non-SRA samples, but some difficulties were encountered

with the high permeability rectangular magnetization loop of the SRA samples. Comparison of loss measurements with J-A model parameters indicates that the parameters that describe the anhysteretic curve have most correlation with measured loss variations. These results imply that further work is required to develop an inverse model with the anhysteretic curve described in terms that have physical interpretations that can be linked to manufacturing processes.

REFERENCES

[1] Y. Kai, Y. Tsuchida, T. Todaka, and M. Enokizono, "Influence of stress on vector magnetic property under rotating magnetic flux conditions," *IEEE Trans Magn.*, vol. 48, no. 4, pp. 1421–1424, 2012.

[2] Y. Kai, Y. Tsuchida, T. Todaka, and M. Enokizono, "Effect of local residual stress in rotating machine core on vector magnetic property," presented at the XIX Int. Conf. Electrical Machines (ICEM), 2010.

[3] M. A. Grande, R. Bidulsky, A. Cavagnino, L. Ferraris, and P. Ferraris, "Investigations on different processing conditions on soft magnetic composite material behavior at low frequency," *IEEE Trans. Ind. Appl.*, vol. 48, no. 4, pp. 1335–1343, 2012.

[4] Z. Gmyrek and A. Cavagnino, "Analytical method for determining the damaged area width in magnetic materials due to punching process," in *Proc. IEEE IECON*, 2011, pp. 1764–1769.

[5] A. Krings, S. Nategh, O. Wallmark, and J. Soulard, "Influence of the welding process on the magnetic properties of a slot-less permanent magnet synchronous machine stator core," in *Proc. XX Int. Conf. Electrical Machines (ICEM)*, 2012, pp. 1331–1336.

[6] D. Jiles and D. L. Atherton, "Theory of ferromagnetic hysteresis," *J. Magn. Magn. Mater.*, vol. 61, pp. 48–60, 1986.

[7] J. V. Leite, N. Sadowski, N. Batistela, and J. P. A. Bastos, "The inverse Jiles-Atherton model parameters identification," *IEEE Trans. Magn.*, vol. 39, no. 3, May 2003.

[8] N. Sadowski and J. P. A. Bastos, *Electromagnetic Modeling by Finite Element Method*. New York, NY, USA: Marcel Dekker, 2003.

[9] P. Kis and A. Ivanyi, "Parameter identification of Jiles-Atherton model with nonlinear least-square method," *Physica B*, vol. 343, pp. 59–64, 2004.

[10] D. C. Jiles, J. B. Thoelke, and M. K. Devine, "Numerical determination of hysteresis parameters for the modelling of magnetic properties using the theory of ferromagentic hysteresis," *IEEE Trans. Magn.*, vol. 28, no. 1, pp. 27–35, Jan. 1992.

[11] J. Izydorczyk, "A new algorithm for extraction of parameters of Jiles and Atherton hysteresis model," *IEEE Trans. Magn.*, vol. 42, no. 10, pp. 3132–3134, Oct. 2006.

[12] D. Lederer, H. Igarashi, A. Kost, and T. Honma, "On the parameter identification and application of the Jiles-Atherton hysteresis model for numerical modelling of measured characteristics," *IEEE Trans. Magn.*, vol. 35, no. 3, pp. 1211–1214, 1999.

[13] E. Del Moral Hernandez, C. S. Muranaka, and J. R. Cardoso, "Identification of the Jiles-Atherton model parameters using random and deterministic searches," *Physica B*, vol. 275, 2000.

[14] R. A. Naghizadeh, B. Vahidi, and S. H. Hosseinian, "Parameter identification of Jiles-Atherton model using SFLA," *COMPEL: Computation and Mathematics in Electrical and Electronic Engineering*, vol. 31, no. 4, 2012.

[15] M. Toman, G. Stumberger, and D. Dolinar, "Parameter identification of the Jiles-Atherton hysteresis model using differential evolution," *IEEE Trans. Magn.*, vol. 44, no. 6, pp. 1098–1101, Jun. 2008.

[16] P. Kis and A. Ivanyi, "Parameter identification of Jiles-Atherton model with nonlinear least-square method," *Physica B*, vol. 343, pp. 59–64, 2004.

[17] F. R. Fulginei and A. Salvini, "Soft computing for the identification of the Jiles-Atherton model parameters," *IEEE Trans. Magn.*, vol. 41, no. 3, pp. 1100–1108, Mar. 2005.

[18] B. Vaseghi, M. E. Mathekga, S. A. Rahman, and A. M. Knight, "Parameter optimization and study of inverse J-A hysteresis model," presented at the IEEE Conf. Electromagnetic Field Computation, CEFC 2012, Oita, Japan, 2012.